Hindawi
Geofluids
Volume 2020, Article ID 8843945, 11 pages
https://doi.org/10.1155/2020/8843945

Research Article

Experimental Study on MICP Aqueous Solution under the Action of Different Organic Substrates

Huai-miao Zheng,[1,2] Ling-ling Wu,[1,2] Kai-wen Tong,[3] Lin Hu,[1,2] Qing Yu,[1,2] Gui-cheng He,[1,2] and Zhi-jun Zhang[1,2]

[1]*School of Resource & Environment and Safety Engineering, University of South China, 421001 Hengyang, China*
[2]*Hunan Province & Hengyang City Engineering Technology Research Center for Disaster Prediction and Control on Mining Geotechnical Engineering, 421001 Hengyang, China*
[3]*University of Chinese Academy of Sciences, 100049 Beijing, China*

Correspondence should be addressed to Zhi-jun Zhang; zzj181@163.com

Received 27 June 2020; Revised 15 August 2020; Accepted 27 August 2020; Published 22 September 2020

Academic Editor: Bo Li

The precipitation rate and cementation strength of calcium carbonate crystals during the process of microorganism-induced calcium carbonate precipitation (MICP) are key factors that affect the application effect of this technology. In order to improve the quality of calcium carbonate formation in the MICP process, egg white protein with a volume fraction of 20%, bovine serum albumin with a mass fraction of 0.3%, sucrose with a mass fraction of 5%, bamboo leaves with a mass concentration of 25 g/L, and bamboo leaf-magnesium chloride ($Mg^{2+}/Ca^{2+} = 4:1$) were added during the experiment of different groups of MICP solutions. The results of the solution test study showed that there was no obvious lag period for bacterial growth under the action of organic matrix. The concentration of bacteria in the reaction solution was higher under the action of sucrose and egg white. The conversion rate of Ca^{2+} under the action of egg white was the fastest, which was about 2.5 times higher than that of the control group. After 14 days of grouting reaction, it was found that the proportion of calcite-type calcium carbonate produced under the action of egg white was the highest, and the Ca element accounted for 66.24% in the solidified material. Sucrose was second; bovine serum albumin was the lowest. The calcium carbonate crystals generated by the control of each organic matrix had a high degree of pore size matching with the tailings under a dry-wet cycle. The structural characteristics of the calcium carbonate crystals, such as crystal form, morphology, and particle size, were mainly due to the interaction between the organic matrix and the calcium carbonate crystals. This study proves that the addition of the organic matrix can improve the formation rate and crystal structure of calcium carbonate during MICP, thus providing a new reference for the development of MICP technology.

1. Introduction

With the enrichment of scientific theories and research methods in geotechnical engineering and the increase of cross-disciplinary interaction, the research on microbial-induced calcium carbonate precipitation (MICP) has attracted wide attention in China and abroad. In recent years, this biochemical reaction has achieved certain results in strengthening soft soil such as loose silt and silty clay, but the cementation effect of calcium carbonate precipitation obtained is not ideal, mainly manifested in a low calcium carbonate crystallization conversion rate, insufficient strength of induced calcium carbonate crystals, and low matching degree between crystal size and interparticle pores [1]. Therefore, based on the principle of the soft template method, this study carried out comparative experiments of MICP aqueous solution under the control of different organic substrates, trying to find an organic matrix that can effectively promote the formation of calcium carbonate in the MICP process. The principle of this method is to use the interaction between the organic matrix and the calcium carbonate cement in geometric lattice matching, stereochemical complementation,

and molecular recognition at specific interfaces to regulate the formation of carbonate composites with specific structures and functions. By improving the crystal form, crystal morphology, and particle size characteristics of the original induced calcium carbonate crystals, it can better exert its material properties in the field of sand reinforcement [2–5].

In the past ten years, domestic and foreign research institutions and scholars had carried out some laboratory studies, mainly using microemulsion, natural biological macromolecules, small molecules, polymers, etc., as soft templates to synthesize calcium carbonate. Mann et al. applied the microemulsion method to the synthesis of calcium carbonate for the first time and synthesized an interesting polycrystalline spongy aragonite structure [6]; Xie and others initially studied the interaction between bovine serum albumin (BSA) and calcium carbonate and found that BSA can promote the nucleation of calcium carbonate crystals, increase the water solubility of calcium carbonate, control the crystallization rate, prevent the generation of amorphous calcium carbonate, and form a highly ordered structure of calcium carbonate, thus inducing and regulating calcium carbonate crystals [7]; Sugawara et al. copolymerized chiral phosphoserine-aspartic acid into polypeptide, inducing the formation of specular spiral calcite [8]. Subsequently, Nishino et al. conducted biomimetic mineralization of $CaCO_3$ at different Mg^{2+} concentrations. The results show that different Mg^{2+} concentrations can significantly change the crystal morphology [9]; Adamiano et al. studied the change of calcium carbonate crystal morphology and kinetics formation process by fluorescence microscopy after alkali treatment of abalone shell green sheet protein fragment (GP) [10]; Wittaya et al. further added different long-chain amino acids such as glycine, 4-aminobutyric acid, and 6-aminocaproic acid to calcium hydroxide suspension, and calcium carbonate prepared by a gas phase diffusion method was transformed from spherical to acicular with the increase of carbon chain length [11]. Under high temperature and high pressure hydrothermal conditions, calcium carbonate crystals were prepared by the urea hydrolysis method with organic carboxylate sodium citrate as an additive. The effects of sodium citrate concentration, ethanol volume fraction, Ca^{2+} concentration, and ionic liquid concentration on the crystal form and morphology of calcium carbonate were investigated [12]. In recent years, Qiao has used egg white protein foam and egg white protein as organic templates to prepare calcium carbonate in different forms by traditional chemical methods [13]; Li used $CaCl_2$ and $(NH_4)_2CO_3$ as raw materials to study the effect of SDBS with different concentrations in solution on the crystallization behavior and morphology of $CaCO_3$ by a gas diffusion method [14].

The above research results show that an organic matrix has the potential to improve MICP technology for strengthening soft soil. As there is few related research on the application of an organic matrix to soft soil at home and abroad at present, in view of this, this paper will initially select the organic matrix with biomineralization and cementation functions as the control template of calcium carbonate crystals. By discussing the influence of different organic matrices on various indexes of calcium carbonate finally induced under the control of different organic matrices and combining with the pore distribution law between tailing sand bodies, it will lay a good foundation for the subsequent solidification research of tailing sand.

2. Test Materials and Devices

2.1. Bacteria and Culture Medium. The bacterium used in this test was Bacillus pasteurianus ii, purchased from the American strain collection center, No. ATCC11859. The bacterium is a facultative anaerobic bacterium. The liquid culture medium used in the test process was CASO+ urea culture medium. Each liter of bacterial culture liquid contains 15 g casein peptone, 5 g soybean peptone, 5 g sodium chloride, 20 g urea, and 1000 mL deionized water, and the pH value is adjusted to 7.3 with 1 M NaOH. Since urea is easy to decompose under high temperature conditions (121°C), urea and other solutions need to be separately sterilized when preparing the medium. The urea solution is subjected to filtration sterilization treatment; other mixed solutions are subjected to high temperature sterilization. After completion, the two are mixed in a septic operation table.

2.2. Preparation of Cementing Fluid. The cementing solution used in this test is a mixture of urea and $CaCl_2$, which mainly provides carbonate ions and calcium sources for the microbial grouting reinforcement process (see formulas (1)–(3)). Based on the previous research of the research group [15, 16], the concentration ratio of urea and $CaCl_2$ in this solution test is 1 : 1, and the specific concentration of both is 0.05 moL/L:

$$Ca^{2+} + \text{Cell} \rightarrow \text{Cell} - Ca^{2+} \quad (1)$$

$$2CO(NH_2)_2 + 2H_2O \rightarrow {CO_3}^{2-} + 2NH^{4+} \quad (2)$$

$${CO_3}^{2-} + \text{Cell} - Ca^{2+} \rightarrow \text{Cell} - CaCO_3\downarrow \quad (3)$$

2.3. Organic Matrix. In order to explore the regulation of different organic substrates on microorganism-induced calcium carbonate crystals, five organic templates, including egg white protein 20%, bovine serum albumin 0.3%, sucrose 5%, bamboo leaves 25 g/L, and bamboo leaves-magnesium chloride ($Mg^{2+}/Ca^{2+} = 4 : 1$), were preliminarily selected by referring to previous accumulated results [17–21].

Among the five selected organic matrices, bovine serum albumin (BSA) is a globulin in bovine serum, which is generally used as a stabilizer in reaction solution. It often plays the role of protection and carrier, can greatly improve the activity of biological cells, and can combine with a variety of cations, anions, and small molecular substances to guide the formation of inorganic substances through biomimetic methods. Egg white mainly contains water and colloidal protein, which is similar to the organic components in pearls, and has low price and good water solubility. It can effectively be used as a carrier to guide the bionic synthesis of calcium carbonate crystals, and the colloidal substance in egg white can enhance the cohesion between sand particles and calcium carbonate cement. The reason why sucrose is used to guide the synthesis of calcium carbonate is that, on the one hand, it can

Table 1: Specific parameters of organic substrates.

Name	Specifications	Content	Manufacturer
Bovine serum albumin (25 g)	Analytic pure AR	BR, 98%	Shanghai Budding Technology Co., Ltd.
Egg white protein (970 g)	Pasteurized egg white	98%	Suzhou Orfu Egg Co., Ltd.
Sucrose (500 g)	Analytic pure AR	99.9%	Tianjin Heyday Xin Chemical Co., Ltd.
Bamboo leaf	Fresh and alive	25 g/L	Picking on campus

decompose and enhance the viscosity between soil particles under high temperature conditions and, on the other hand, it can effectively prepare calcium carbonate crystals with specific structures. Bamboo leaves are gramineous plants and are rich in manganese, iron, copper, nickel, selenium, silicon, and other trace elements and other organic matters. Relevant studies [22] show that the organic components extracted from natural bamboo leaves can control the crystal form and morphology of synthesized calcium carbonate crystals. At the same time, amorphous calcium carbonate (ACC) can be kept in a stable state for a long time under the coordinated control of magnesium ions. The method of using natural plants to control bionic calcium carbonate is convenient to operate, and also, the product is environment-friendly and pollution-free. The egg white used in the experiment can be directly separated from fresh eggs, but because the separated egg white is very inconvenient to sterilize, this experiment uses the commercially available bottled pasteurized egg white liquid. The specific specifications and parameters of each organic matrix are shown in Table 1.

2.4. Test Physical Devices. In order to meet the test conditions of convenient sampling, waterproof device, aseptic reaction, oxygen supply, and ventilation, a new MICP technology solution test reaction device was designed in this study. The main body of the device is made of high borosilicate glass. The overall height of the device is 22.5 cm, and the inner diameter is 10 cm. The main structure consists of upper and lower reaction vessels. A circular rubber water stop ring is arranged between the two parts. The upper and lower structures are firmly connected by steel rings. The reaction vessel at the upper part of the device comprises a plurality of basic structures such as an oxygen supply port, a grouting port, a liquid discharge port, and the like. In order to avoid serious blockage of the liquid discharge port caused by generated tiny calcium carbonate crystals, a permeable gauze with tiny pore diameter is arranged at the inner side of the liquid discharge port at the upper part of the device. In the lower reaction vessel, the bottom is a solid member, and the bottom is covered with eggshells ($10\,g \pm 0.1\,g$) with uniform size, so that calcium carbonate crystals generated in the reaction are organically connected into a whole, which is convenient for final cutting and sampling. The physical model device used in the test is shown in Figure 1.

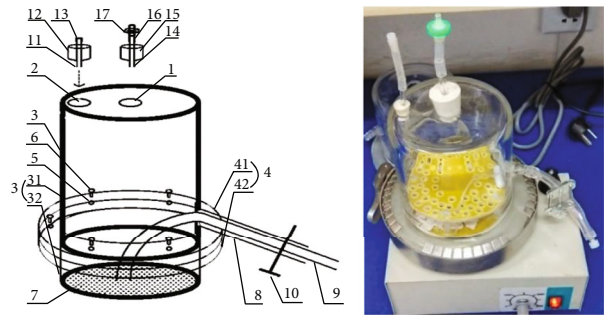

Figure 1: Structure of the reaction device in the solution test.

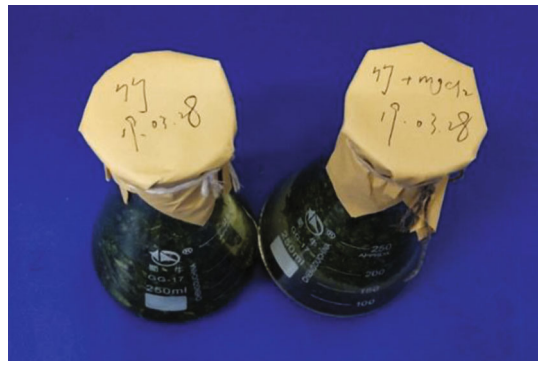

Figure 2: Extraction of chlorophyll from bamboo leaves.

3. Test Methods

3.1. Preparation and Extraction of Organic Matter Such as Chlorophyll from Bamboo Leaves. Fresh and tender green bamboo leaves are picked in the campus, stems from the bamboo leaves are removed, the bamboo leaves are cleaned with ultrapure water for 2-3 times, the bamboo leaves are dried in a drying oven at 30°C for 20 minutes, the bamboo leaves are soaked in 0.07% $CuSO_4$ solution for 5 hours, the bamboo leaves are washed with ultrapure water for 3-4 times, and the bamboo leaves are dried to constant weight. Then, the dried bamboo leaves are cut and poured into ultrapure water just above the surface of the bamboo leaves for water bath treatment and filtered by a filter funnel; the filtrate is subjected to reduced pressure distillation operation to a semifluid state and finally is cooled to room temperature and stored in a conical flask [23–25], as shown in Figure 2.

3.2. Preparation and Sampling of Powdered Calcium Carbonate Cements. After the solution test reaction is finished, the calcium carbonate gel on the support body is scraped into a culture dish with a knife and tweezers, put into a drying box to dry at 50°C for 2-3 days after the sampling is finished, weighed to constant weight, poured into a grinder, and ground repeatedly and evenly, and then, fine powder samples were taken through a 300-target screen for SEM, XRD, TEM, and other tests.

3.3. MICP Solution Test under the Control of Organic Matrix

3.3.1. Test Methods. This study is a MICP aqueous solution test under the action of the organic matrix. Five organic matrices, including egg white protein, bovine serum albumin, bamboo leaves, sucrose, bamboo leaves-magnesium chloride, which have obvious regulatory effects on the crystal form and crystal habit of calcium carbonate crystals, are selected. Six experimental groups including the control group (without adding any organic matrix) are set up. Under the conditions of temperature of 30°C, initial pH of 7.3, initial OD_{600} of 2.0, and stirring rate of 150 rpm, the grouting test was started. Considering the actual size of the device and the amount of sample liquid required for each detection item, the grouting volume of each reaction liquid in the test was the following: 15 mL of bacterial liquid, 200 mL of culture medium, 100 mL of calcium chloride solution, 100 mL of urea solution, and 100 mL of organic matrix solution (the control group was ultrapure water). After the solution in the device was drained out every 24 hours, a new round of reaction slurry was poured by a peristaltic pump. During the test reaction, the change rule of each index (bacterial concentration, pH, Zeta potential, dissolved oxygen, calcium ion concentration) in the reaction solution within 1 d was measured, and the monitoring time interval was 2 h. After the grouting period reaches 14 days, the reaction liquid is discharged, the fixed steel ring is opened, the upper and lower structures of the separation device are disassembled, and the sample is put into a drying box (60°C) for drying for 24 hours, and then, the solidified sample is taken out and tested by SEM, XRD, and other items, and the test results of the six experimental groups are compared qualitatively and quantitatively.

3.3.2. Determination of Bacterial Quantity. The measurement of the number of bacteria is realized by detecting the absorbance of the bacterial solution. The measuring equipment is a protein nucleic acid analyzer (Eppendorf Company of Germany, model number is BioPhotometer). In the experiment, 5 mL of reaction supernatant is taken from the device every 2 hours to measure the OD_{600} value of the bacterial suspension. The obtained value is substituted into the following formula for conversion to obtain the actual number of bacteria in the reaction solution [26]:

$$Y = 8.59 \times 10^4 Z^{1.3627}. \quad (4)$$

In the formula, Z is OD_{600} value and Y is bacterial concentration (units/μL^{-1}). This formula can only be used when the value of OD_{600} is within the range of 0.2~0.8. If it is beyond this range, it needs to be diluted before conversion.

3.3.3. pH Value. Every 2 hours, 100 mL of the reaction solution is taken into a conical flask, and the change of the pH value of the reaction solution within 1 day is observed by using a diamagnetic precision desktop pH meter (HACH Company of the United States, model HQ411D).

3.3.4. Monitoring of Dissolved Oxygen in Solution. Dissolved oxygen in the reaction solution is very important to the life activities of microorganisms. In this experiment, a 100 mL centrifuge tube is used to contain 80 mL of reaction solution in different reaction periods. The dissolved oxygen in the solution in one day is monitored by a convenient dissolved oxygen meter (China Guangzhou Jinhe Technology Testing Co., Ltd., model 958787-1KTOK).

3.3.5. Zeta Potential. The stability of colloidal dispersion in the reaction liquid system before and after the addition of the organic matrix was judged by the variation of Zeta potential. The Zeta potential value in the solution was monitored every 2 hours during the experiment. Monitoring equipment was the Zeta potential measuring instrument (JS94HK, China Beijing Zhongyi Kexin Technology Co., Ltd.). The approximate relationship between Zeta potential and stability of the solution system is shown in Table 2 [27].

3.3.6. Determination of Ca^{2+} Concentration. Regularly, the discharged solution from the device was collected, made to pass through a 0.22 μm filter and dropped into a 20 mL centrifuge tube, and measured according to "EDTA Titration of Calcium in Water Quality" GB 7476-87.

3.3.7. Microstructure Test. In order to analyze the microstructure of the generated samples, the ground and dried calcium carbonate cemented samples were analyzed by scanning electron microscopy (FEI-F50 test field emission scanning electron microscopy) to observe the morphological characteristics of calcium carbonate samples generated under different organic substrates. Then, typical powdered samples were selected for XRD detection (X-ray diffractometer model SMARTLAB9) and FT-IR testing (FT-IR testing Fourier infrared spectrometer model Nicolet), respectively, and then, the crystal form and composition of calcium carbonate samples were obtained.

4. Results and Discussion

This solution test mainly detects and analyzes the change rule of bacterium quantity, pH value, Zeta potential, dissolved oxygen, and calcium ion concentration in the reaction solution of each experimental group within 24 hours, and the composition, crystal form, morphology, and particle size of the carbonate gel were compared and analyzed. Figure 3 shows the effect of dismantling the device after the test.

4.1. Changes in the Number of Bacteria in Reaction Solution. The change curve of bacterial number in Figure 4 shows that the bacterial number in the reaction solution under the control of the five organic substrates shows an obvious upward trend within one day. The bacterial growth basically conforms to the gong bozi-Richard model, and there is no obvious lag period. This may be due to the nutrient components such as the carbon source, nitrogen source, and the like required by microorganism's life activities in the culture medium of the reaction solution. The microorganism continuously absorbs the nutrient substances in the surrounding environment under the stirring action, so that the cells grow and multiply rapidly, thus increasing the bacterial concentration in the reaction solution.

Table 2: Relationship between Zeta potential and solution system stability.

Zeta potential	Colloidal stability
0~±5	Rapid condensation or condensation
±10~±5	Began to be unstable
±30~±40	General stability
±40~±60	Better stability
>±61	Excellent stability

Among them, the bacterial concentration of the reaction solution under the control of sucrose and egg white increased rapidly, reaching about 160,000/μL at 24 hours. Compared with other organic substrates, it played a better role in promoting bacterial growth, which was related to the organic matter contained in egg white protein and sucrose itself and could be better absorbed by bacterial cells. However, no organic substrate was added in the blank control group, and its bacterial activity was slightly lower than that of the other four. Its cell concentration is only 101,000 cells/μL, which indicates that egg white protein, sucrose, and other organic substrates are rich in nutrients required by the life activities of Bacillus pasteurianus, thus significantly enhancing its bacterial activity, promoting bacterial growth and division, enabling it to grow faster in one day, with higher urease activity, and always at the logarithmic growth stage of bacterial growth, providing a better reaction basis for urea hydrolysis.

4.2. pH Change. The change rule of pH in Figure 5 shows that the pH value of the reaction solution in each experimental group rises rapidly within 0-12 h, mainly due to the higher urease activity of bacteria in this stage, which can effectively hydrolyze urea in the solution and generate ammonium ions, thus continuously increasing the pH value in the reaction solution. However, when urea is completely hydrolyzed, the pH value in the reaction solution will gradually stabilize, and the change rule of pH value in each experimental group shown in the figure is basically the same. The pH value of the reaction solution in the other experimental groups was basically stable at 9.0 in the 20-24 h period except the pH value in the bamboo leaf+magnesium chloride control group. This is because magnesium chloride will ionize into Cl^- and Mg^{2+} after hydrolysis and combine with H^+ and OH- in water to form HCl and $Mg(OH)_2$, of which $Mg(OH)_2$ is a weak base, so the overall pH value is slightly acidic, resulting in a lower pH value compared with the other five reaction liquid phases.

4.3. Change of Dissolved Oxygen in Reaction Solution. As can be seen from Figure 6, the dissolved oxygen of the reaction solution in the six groups of experiments decreased with the increase of time, which indicates that the growth and metabolism of microbial cells need to consume oxygen continuously. Except for egg white and bamboo leaf+magnesium chloride groups, the dissolved oxygen of the solution in the other four groups of experiments decreased slowly within 0~8 hours, at which time the bacterial growth was in the lag phase, so the bacterial growth was slower. Within 8~18 h, the dissolved oxygen decreased rapidly due to the logarithmic phase of bacterial growth. However, the microbial activity was still relatively high within 22~24 hours, but the oxygen content in the solution was seriously insufficient, so it gradually stabilized.

4.4. Zeta Potential. The curve change in Figure 7 shows that the Zeta potential of the reaction solution in each experimental group is always negative, so negative particles dominate the reaction process of the solution within 24 hours. Most of its potentials rose from -15 mV to -0.5 mV, which shows that the dispersed particles in the solution are unstable at the beginning of the reaction stage due to the continuous combination of Ca^{2+} and CO_3^{2-}. As time increases, the metabolism of microorganisms accelerates, which increases urease activity. Urease accelerates the hydrolysis of urea and continuously generates CO_3^{2-}. The dispersed particles in the solution tend to agglomerate, the attraction force is greater than the repulsive force, and the accumulated amount of calcium carbonate cementation increases due to the destruction of dispersion. The Zeta potential of the solution under the regulation of egg white and sucrose approaches zero at the 16th hour, which is related to the number of bacteria in the solution and the conversion rate of calcium ions. When it reaches 24 h, the potential values of all experimental groups approach zero, at which time the calcium ions in the solution are basically converted.

4.5. Ca^{2+} Concentration. From the change data in Figure 8, it can be seen that the calcium ion concentration in the sample solution in each experimental group shows a downward trend within 0~20 h, and the conversion basically ends at 20 h. The decrease gradient of calcium ion concentration in the egg white protein group is the largest. Compared with the blank control group, the conversion rate of calcium ion in the egg white protein group is increased by about 2.5 times at the same time, mainly due to the rapid increase of bacterium number and the increase of urea hydrolysis rate by urease, which greatly improves the binding rate of calcium ion with carbonate and bicarbonate ions and increases the precipitation rate of calcium carbonate.

4.6. Microstructure. Figure 9 is a scanning electron microscope view of calcium carbonate gel induced by microorganisms under the control of different organic substrates, wherein Figure 9(a) is an enlarged view of deposited calcium carbonate crystals under the condition of the blank control group, i.e., without adding any organic substrates. From the figure, it can be seen that the main form of calcium carbonate is a mixture of calcite and vaterite, and the induced particle size distribution is uneven, with the particle size ranging from 1.3 μm to 25.49 μm. Figure 9(b) is a microscopic particle diagram of calcium carbonate under the control of bovine serum albumin. The crystal particles are relatively uniform, mainly vaterite, and the particle size is basically about 5.30 μm m. Figure 9(c) is an SEM image of the calcium carbonate crystal product under the control of sucrose, which is mainly composed of spherical and square crystal particles, showing a layered structure, and the particle size range of the

(a) Calcium carbonate on the support plate

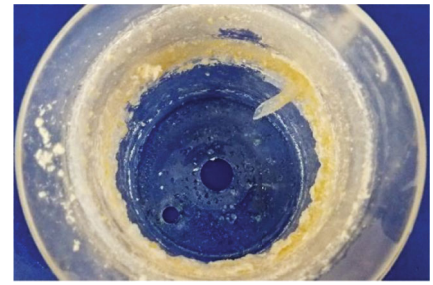

(b) Calcium carbonate gel on the inner wall of the device

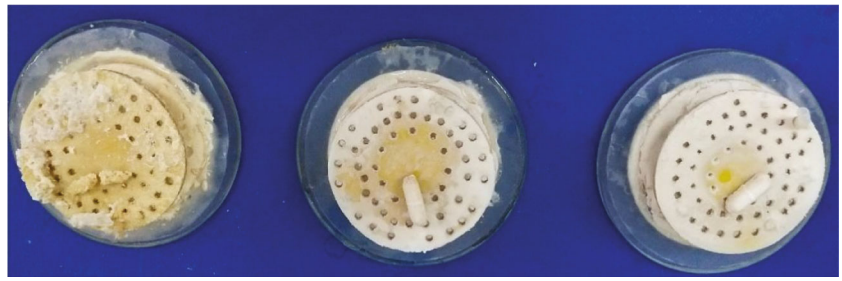

(c) Calcium carbonate products at the bottom of the device after being regulated by different organic templates

Figure 3: Calcium carbonate sample after device removal.

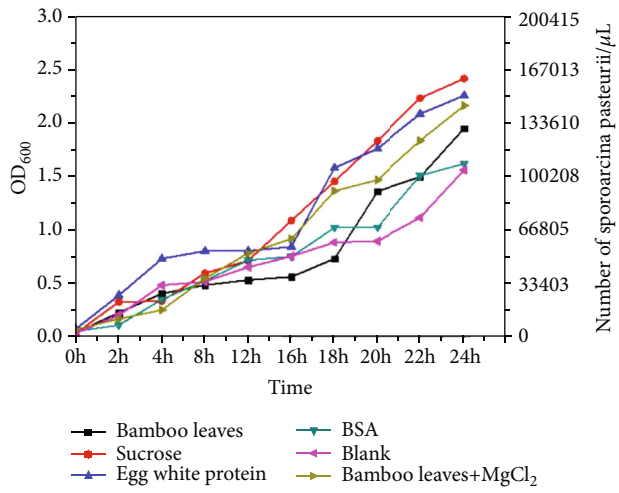

Figure 4: Variation chart of bacterium number.

particles can reach 1.8 μm to 4.67 μm. Figure 9(d) shows the crystal morphology under the control of bamboo leaves. Most of them are regular and uniform rhombus crystal structures. When $MgCl_2$ with a concentration of 2 mol/L is added, the crystal structure changes to multiangular crystal and gradually evolves into an oval state (Figure 9(e)). Figure 9(f) is a microscopic view of calcium carbonate gel crystals under the control of egg white protein. Compared with induced crystals in other experimental groups, calcium carbonate crystals in this group are more closely linked. The main form of calcium carbonate shown in the figure is calcite crystals with a particle size of 2.0 μm~10 μm, which are mostly firmly bonded to each other through fiber substances of egg white. Since the pore sizes of tailings are mostly distributed between 0 and 40 μm under the dry-wet cycle state, the cementation form between tailing particles is mainly the accumulation connection between calcium carbonate crystals under the control state of the above experimental group.

Through further analysis of the elemental state of calcium carbonate gel in each experimental group (point-scanning energy spectrum, Figure 10), it is found that in the elemental analysis shown in Figure 10(a), Ca and O have larger peaks, while the peaks of Cl, N, C, and other elements are lower, which indicates that the main elements of calcium carbonate gel in the blank experimental group are Ca, O, Cl, N, and C, which are the basic constituent elements in the reaction liquid, and the specific proportions of each element are 35.06%, 42.35%, 7.95%, 8.64%, and 6.00%. Compared with Figure 10(b), Sr element is missing, which is related to the main components in BSA. The counting rate of other overlapping elements is obviously lower, which indicates that the detected Ca, O, and other signals in Figure 10(b) are stronger and more reliable, and the proportions of Ca, O, Cl, N, C, and Sr elements are 55.42%, 33.26%, 3.12%, 3.86%, 4.14%, and 0.21%, respectively. On the basis of Figure 10(a), Figure 10(c) contains trace elements such as Mg, Na, Al, Si, Cu, and Ni. Similarly, the counting rate of Ca, O, and other elements in the cements of this group is higher than that of the blank group, with the total proportion of Ca and O elements reaching 81.12%. The element distribution (Figure 10(d)) of calcium carbonate gel under the control of bamboo leaves shows that the elements P, Na, Cu, Zn, and the like contained in bamboo leaves are combined with calcium carbonate crystals, and the content of Ca in the cement is as high as 47.6%. In the synergistic regulation of $MgCl_2$, the content of Mg element in gel is 6.90%, and the content of Ca element is increased by 8.66%. In Figure 10(f), the calcium carbonate cement under the action of egg white has the highest content of Ca, up to 66.24%.

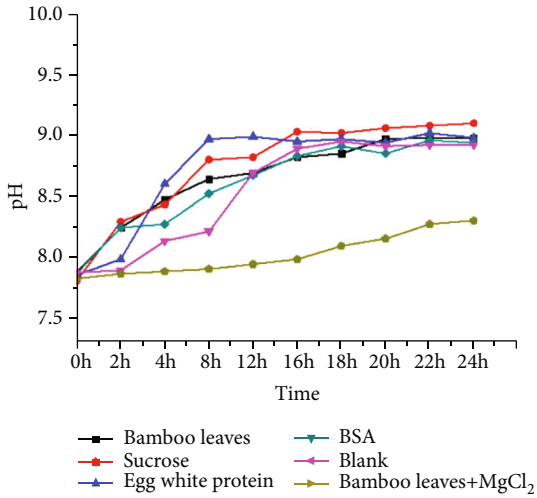

Figure 5: pH change diagram of reaction solution.

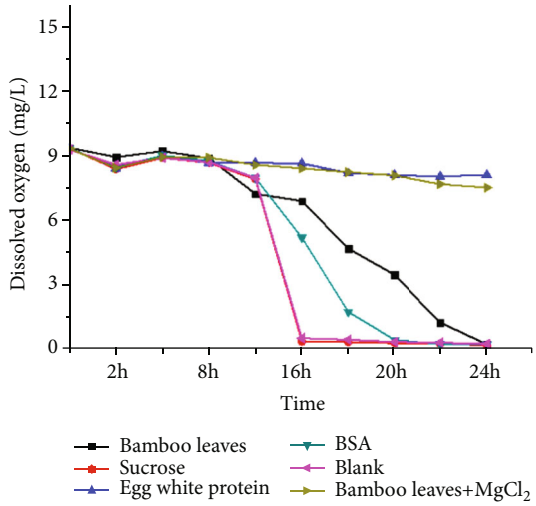

Figure 6: Change chart of dissolved oxygen.

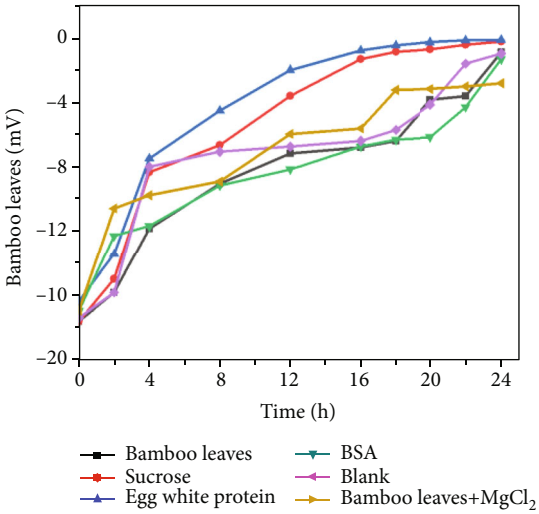

Figure 7: Zeta potential value change diagram.

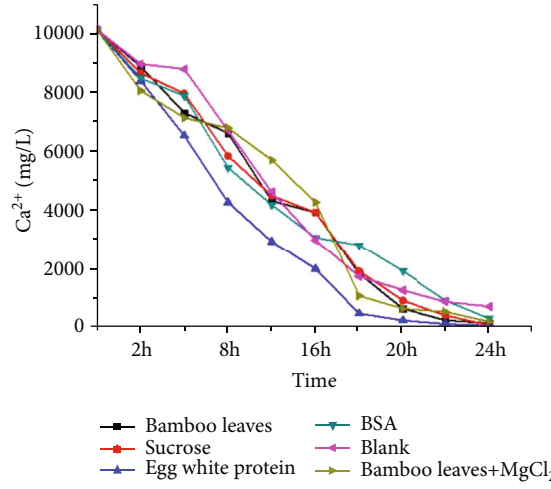

Figure 8: Change chart of calcium ion concentration.

Meanwhile, the S, Al, Mg, Ca, O, N, and other elements rich in egg white coordinate with each other to form calcium carbonate gel.

4.7. Crystal Form and Composition Analysis of Calcium Carbonate. XRD tests were carried out on calcium carbonate mineralized samples under the control of different organic substrates, and the results are shown in Figure 11. By comparing the relevant data of the PDF standard card, it can be found that the calcium carbonate sample in the control group is a mixture composed of calcite and vaterite. The diffraction angle positions of calcite crystal are 2 = 23.0, 29.4, 35.9, 39.5, 43.1, 47.5, 48.5, and 57.4, respectively, corresponding to (012), (104), (110), (113), (202), (018), (116), and (122) crystal planes. However, the diffraction angle of vaterite crystal is around 2 = 24.8, 26.9, 32.7, and 43.8, corresponding to (110), (112), (114), and (300) crystal planes, respectively. Most of the samples under BSA regulation are mainly vaterite crystal form ((110) crystal plane) but are still doped with a little calcite ((104) crystal plane). XRD patterns detected in three groups of experimental samples of sucrose, bamboo leaves, and egg white protein show that calcium carbonate induced is calcite type ((104) crystal plane). The calcium carbonate sample produced by adding $MgCl_2$ to bamboo leaves is still a mixture of calcite and vaterite.

In order to further quantify the molar ratio of calcite and vaterite contained in the product, the data of the above three groups of experimental samples were calculated according to the following formula:

$$\frac{I^{104}_{c}}{I^{110}_{v}} = 7.619 \times \frac{X_c}{X_v}. \quad (5)$$

In the formula, the ratio of the diffraction peak integral intensity of calcite and vaterite in the mixture is expressed; 7.619 is the proportional constant; and X_c/X_v is the ratio of the amount of calcite to vaterite in the mixture.

Calculations show that the molar ratios of calcite to vaterite in the blank group, BSA group, and bamboo leaf+$MgCl_2$ experimental group are 2.736, 0.894, and 0.615, respectively.

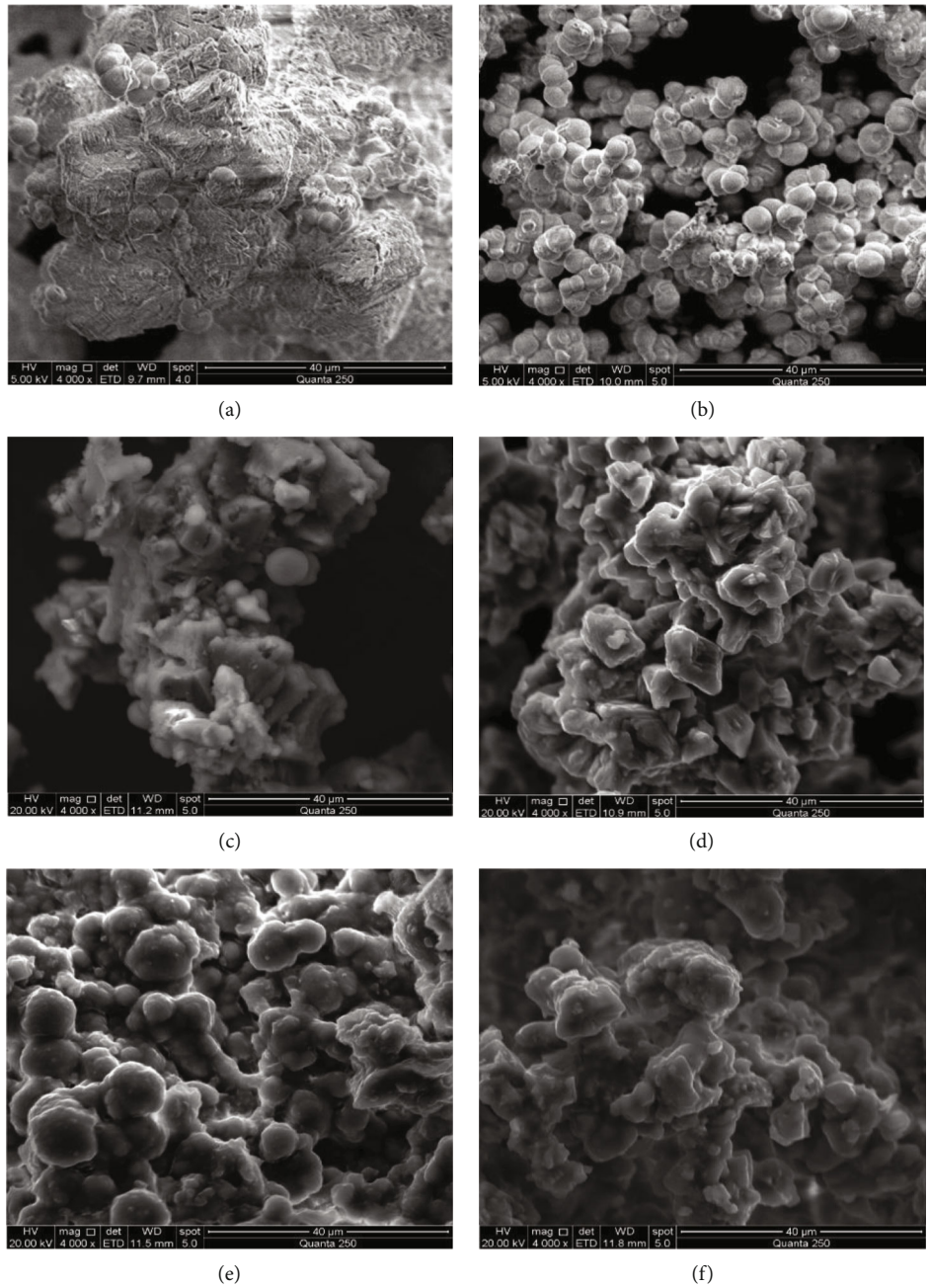

Figure 9: SEM images of cements of each experimental group (magnification: 4000), reaction concentration: blank group (a); (b) BSA with mass fraction of 0.3%; (c) sucrose with a mass fraction of 5%; (d) bamboo leaves with a mass concentration of 25 g/L; (e) the mass fraction of bamboo leaves is 25 g/L + 2 mol/L $MgCl_2$; (f) 20% egg white protein by volume.

Therefore, the above-mentioned preliminarily screened organic matrix has obvious regulation effect on the crystal form of induced calcium carbonate crystal.

According to the infrared spectrum shown in Figure 12, calcium carbonate samples in the blank group have characteristic absorption peaks at 3419.79 cm^{-1}, 2509.39 cm^{-1}, 1406.83 cm^{-1}, 1076.28 cm^{-1}, 878.68 cm^{-1}, and 711.73 cm^{-1}. Among them, the absorption peaks of 2509.39 cm^{-1} and 3419.79 cm^{-1} are mainly caused by symmetric stretching vibration and asymmetric stretching vibration of O-H bond, which are mainly due to the existence of hydroxyl groups and adsorbed water of calcium carbonate particles, while 711.73 cm^{-1} and 878.68 cm^{-1}, respectively, correspond to the characteristic absorption peaks of calcite crystal at V_4 and V_2; the peak at V_2 is strong and sharp; and 1076.28 cm^{-1} corresponds to the absorption peak at V_4 of vaterite crystal, so the detection results are consistent with XRD, and the calcium carbonate crystals in the blank group are aragonite and calcite crystal. When BSA was added, the out-of-plane bending vibration peak (878.68 cm^{-1}) of calcium carbonate shifted to the low wave number direction (873.75 cm^{-1}), which indicated that the interaction between BSA and

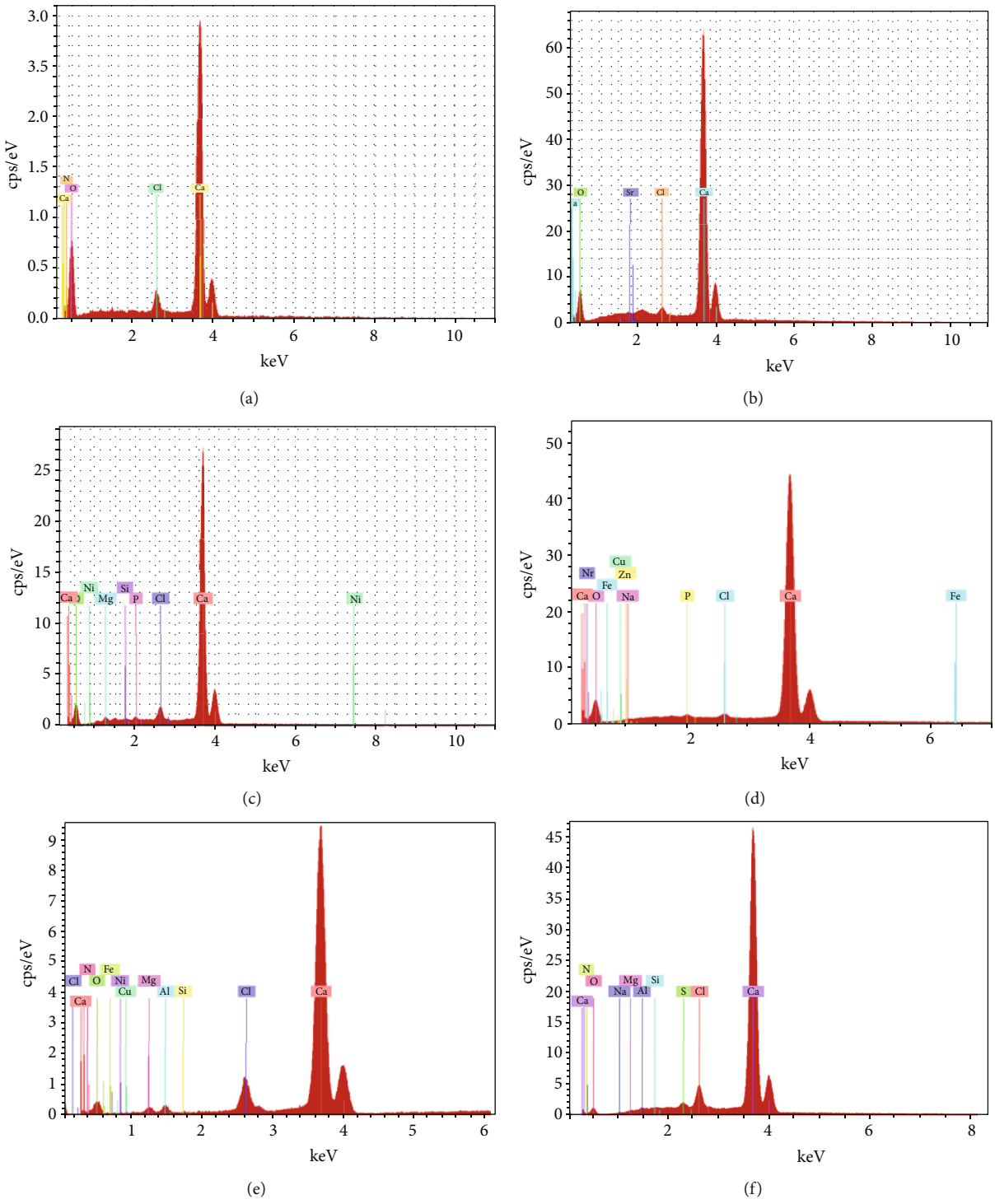

Figure 10: Energy spectrum analysis of cement. The energy spectrum analysis chart of the calcium carbonate cement deposited in each experimental group: (a) blank group; (b) BSA; (c) sucrose; (d) bamboo leaves; (e) bamboo leaves+$MgCl_2$; (f) egg white protein.

calcium carbonate changed the form of O-C-O. The absorption peaks at 873.75 cm^{-1}, 711.73 cm^{-1}, and 1076.28 cm^{-1} still indicated that the calcium carbonate in the sample was calcite type and vaterite type. The infrared spectra of the samples in the bamboo leaf+magnesium chloride experimental group show absorption peaks at 874.19 cm^{-1} and 712.15 cm^{-1}, so the calcium carbonate samples obtained are also the mixture of calcite and vaterite. From the infrared spectra of sucrose, bamboo leaves, and egg white, it can be seen that there are absorption peaks at 878 cm^{-1} and 710 cm^{-1}, which indicates that the experimental sample is calcite type, and the egg white group moves 20 cm^{-1} and 10 cm^{-1} towards high wave displacement at 3419.79 cm^{-1} and 1406.83 cm^{-1}, respectively, on the basis of the blank group, indicating that there is a strong interaction between egg white protein and calcium carbonate.

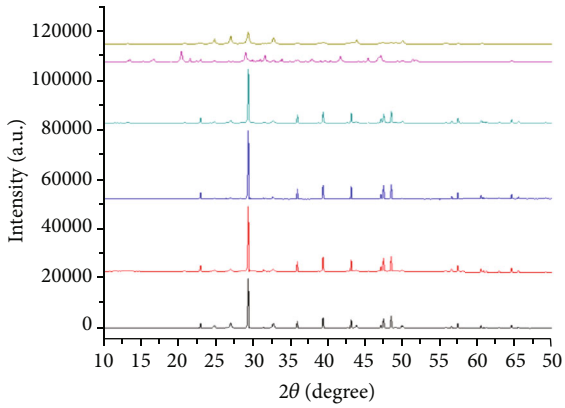

Figure 11: XRD test of cement samples.

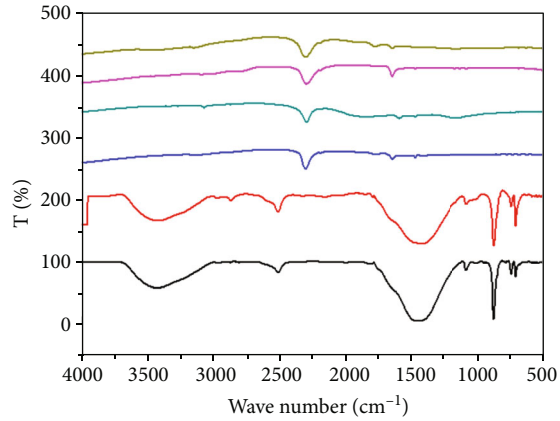

Figure 12: FT-IR test of cement samples.

5. Conclusion

In this paper, the number of bacteria, pH value, dissolved oxygen, Zeta potential value, and Ca^{2+} concentration in the reaction solution were detected and analyzed through MICP aqueous solution tests under the control of five different organic substrates. The microstructure characteristics of calcium carbonate cements generated by the control of various organic substrates were compared and studied, and the following main conclusions were obtained:

(1) The five organic substrates, egg white, bamboo leaves, sucrose, and bovine serum albumin, can significantly enhance the urease activity of Bacillus Pasteurella. Among them, egg white and sucrose have the highest contribution to the growth and reproduction of Bacillus Pasteurella cells. The change of dissolved oxygen in the reaction solution is directly proportional to the concentration of bacteria. The dissolved oxygen decreases fastest in 8~18 h and tends to be stable in 22~24 h. With the continuous progress of the reaction, except for the effect of bamboo leaves and magnesium chloride, the pH value of the reaction solution in each experimental group will gradually stabilize at 9.0 in the period of 20~24 hours

(2) Negative particles in the reaction solution in each experimental group are dominant. With the increase of time, Ca^{2+} and CO_3^{2-} in the solution tend to coagulate continuously, and the coagulation rate under the regulation of egg white and sucrose is the fastest. When reaching 24 h, the potential value of each experimental group is close to 0. The calcium ion concentration showed the same change trend, and the calcium ion conversion rate of the egg white protein group was the highest, which was about 2.5 times higher than that of the control group

(3) The above-mentioned five organic substrates have significant regulation effect on the crystal form, crystal appearance, and particle size characteristics of calcium carbonate crystals induced by MICP technology. Under the action of 5% sucrose, 25 g/L bamboo leaves, and 20% egg white protein, the above-mentioned five organic substrates are easy to be all calcite calcium carbonate, and the calcium carbonate cement under the action of egg white has the highest Ca content, which can reach 66.24%. In addition, the changes in the structural characteristics of calcium carbonate crystals are mainly due to the strong interaction between the organic matrix and calcium carbonate crystals

Data Availability

All data used in this study can be obtained by contacting the corresponding author (Zhang Zhi-jun), email address: zzj181@163.com.

Conflicts of Interest

The authors declare no conflicts of interest related to the publication of this paper.

Authors' Contributions

Wu Ling-ling and Zheng Huai-miao contributed equally to this work.

Acknowledgments

This study was supported by the National Natural Science Foundation of China (51804164, 51774187, and 51974163), the Natural Science Foundation of Hunan Province (2019JJ50498 and 2017JJ3274), and the Scientific Research Foundation of Hunan Provincial Education Department (18B276 and 17A184). Thanks to the Hunan Province & Hengyang City Engineering Technology Research Center for Disaster Prediction and Control on Mining Geotechnical Engineering (2019TP2070) for providing experimental platform support.

References

[1] C. X. Qian, A. H. Wang, and X. Wang, "Advances of soil improvement with bio-grouting," *Rock and Soil Mechanics*, vol. 36, no. 6, pp. 1537–1548, 2015.

[2] D. Walsh and S. Mann, "Fabrication of hollow porous shells of calcium carbonate from self-organizing media," *Nature*, vol. 377, no. 6547, pp. 320–323, 1995.

[3] W. K. Zhu, X. G. Luo, X. Y. Lin, J. Zhou, and Y. Lu, "Effects of temperature on the crystallization of calcium carbonate in egg white protein solution system," *Materials Science Forum*, vol. 675-677, no. 1, pp. 349–352, 2011.

[4] H. Tong, W. Ma, L. Wang, P. Wan, J. Hu, and L. Cao, "Control over the crystal phase, shape, size and aggregation of calcium carbonate via a L-aspartic acid inducing process," *Biomaterials*, vol. 25, no. 17, pp. 3923–3929, 2004.

[5] Z. Wang, N. Zhang, J. Ding, C. Lu, and Y. Jin, "Experimental study on wind erosion resistance and strength of sands treated with microbial-induced calcium carbonate precipitation," *Advances in Materials Science and Engineering*, vol. 2018, 10 pages, 2018.

[6] S. Mann, B. R. Heywood, S. Rajam, and J. D. Birchall, "Controlled crystallization of $CaCO_3$ under stearic acid monolayers," *Nature*, vol. 334, no. 6184, pp. 692–695, 1988.

[7] A. J. Xie, Y. H. Shen, S. Y. Zhang, and F. X. Xie, "Study on the interaction between bovine serum albumin and calcium carbonate in physiological saline," *Journal of Inorganic Chemistry*, vol. 4, 607 pages, 2001.

[8] T. Sugawara, Y. Suwa, K. Ohkawa, and H. Yamamoto, "Chiral biomineralization: mirror-imaged helical growth of calcite with chiral phosphoserine copolypeptides," *Macromolecular Rapid Communications*, vol. 24, no. 14, pp. 847–851, 2003.

[9] Y. Nishino, Y. Oaki, and H. Imai, "Magnesium-mediated nanocrystalline mosaics of calcite," *Crystal Growth & Design*, vol. 9, no. 1, pp. 223–226, 2009.

[10] A. Adamiano, S. Bonacchi, N. Calonghi et al., "Structural changes in a protein fragment from abalone shell during the precipitation of calcium carbonate," *Chemistry - A European Journal*, vol. 18, no. 45, pp. 14367–14374, 2012.

[11] W. Chuajiw, K. Takatori, T. Igarashi, H. Hara, and Y. Fukushima, "The influence of aliphatic amines, diamines, and amino acids on the polymorph of calcium carbonate precipitated by the introduction of carbon dioxide gas into calcium hydroxide aqueous suspensions," *Journal of Crystal Growth*, vol. 386, pp. 119–127, 2014.

[12] Y. F. Gao, *Study on the Crystal Form and Morphology of Calcium Carbonate Controlled by Sodium Citrate*, South China University of Technology, 2015.

[13] Z. Qiao, *Preparation of Bionic Calcium Carbonate by Egg White Template Method and Its Adsorption Properties [D]*, Southwest University of Science and Technology, 2017.

[14] M. W. Li, *Study on Crystallization Behavior of Calcium Carbonate Controlled by Sodium Dodecylbenzene Sulfonate Template [D]*, Jilin University, 2018.

[15] L. L. Wu, Z. J. Zhang, Q. Yu, Y. X. Pan, and L. Hu, "Improvement of the tailings properties in a metal mine by microbiological grouting," *Journal of China University of mining&Technology*, vol. 47, no. 6, pp. 1354–1359, 2018.

[16] R. Gui, Y.-X. Pan, D.-X. Ding, Y. Liu, and Z.-J. Zhang, "Experimental study on the fine-grained uranium tailings reinforced by MICP," *Advances in civil engineering*, vol. 2018, 10 pages, 2018.

[17] A. M. Ding, H. Luo, M. Cheng, J. M. Zhu, and J. C. Yao-Biomimetic synthesis of calcium carbonate controlled by egg white protein and semipermeable membrane," *Journal of Analytical Testing*, vol. 31, no. 6, pp. 696–699, 2012.

[18] Z. J. Zhang, K. W. Tong, H. Lin, Y. Qing, and L. L. Wu, "Experimental study on solidification of tailings by MICP under the regulation of organic matrix," *Construction and Building Materials*, vol. 265, p. 120303, 2020.

[19] Y. P. Wu, *Preparation and Characterization of Calcium Carbonate by Plant Template Method*, Anhui University, 2009.

[20] R. Lakshminarayanan, X. J. Loh, S. Gayathri et al., "Formation of transient amorphous calcium carbonate precursor in quail eggshell mineralization: an in vitro study," *Biomacromolecules*, vol. 7, no. 11, pp. 3202–3209, 2006.

[21] Z. X. Chen, *Application of Histidine Modified Chitosan in Biomimetic Synthesis and Protein Isolation [D]*, overseas Chinese university, 2014.

[22] Y. P. Wu and A. J. Xie, "Research progress on calcium carbonate biomineralization-soft template regulation," *Journal of Anqing Teachers (Natural Science Edition)*, vol. 15, no. 1, pp. 78–80, 2009.

[23] Z. D. Zulkafli, H. Wang, F. Miyashita, N. Utsumi, and K. Tamura, "Cosolvent-modified supercritical carbon dioxide extraction of phenolic compounds from bamboo leaves (Sasa palmata)," *The Journal of Supercritical Fluids*, vol. 94, pp. 123–129, 2014.

[24] J. Xie, Y. S. Lin, X. J. Shi, X. Y. Zhu, W. K. Su, and P. Wang, "Mechanochemical-assisted extraction of flavonoids from bamboo (Phyllostachys edulis) leaves," *Industrial Crops and Products*, vol. 43, pp. 276–282, 2013.

[25] S. Shen, J. L. Duan, Y. Li, C. Wang, J. J. Fu, and H. B. Wang, "Study on extraction technology and functional application of chlorophyll from bamboo leaves," *New Chemical Materials*, vol. 46, no. 1, pp. 117–120, 2018.

[26] X. Zhao, *Experimental study on microbial induced calcium carbonate precipitation (MICP) solidification of soil*, China University of Geosciences, 2014.

[27] M. Yu, A. M. Lu, X. T. Li, G. Z. Li, and R. Peng, "Study on influencing factors of Zeta potential in carbonate rocks," *Science, Technology and Engineering*, vol. 16, no. 20, pp. 165–168, 2016.